

Chapter II

COLOR RECOGNITION FOR TEMPERATURE MEASUREMENTS ON LIQUID CRYSTAL COATED HEAT TRANSFER SURFACES

Cengiz Camci

THE PENNSYLVANIA STATE UNIVERSITY
Department of Aerospace Engineering

Summary

List of Symbols

II . 1 Color Vision Principles for Liquid Crystal Image Interpretation

II . 2 The Present Hue Capturing System

II . 3 The Model for Hue versus Temperature Calibrations

II . 4 Hue Calibration Results and Discussion

Hue versus Temperature Relation

Effect of Illumination Source on Hue versus Temperature Calibration

Spatial Distribution and Repeatability of Liquid Crystal Color Response

Hue versus Intensity

Isotherm Extraction from a Typical Liquid Crystal Image

II . 5 Conclusions

References

Summary

This chapter describes an image processing based color-capturing technique for the quantitative interpretation of liquid crystal images used in convective heat transfer studies. The principles of color perception/reproduction and the imaging system are discussed in detail. The hue versus temperature relation is determined experimentally. The repeatability of the new hue-

capturing process and the effects of the strength of the light source illuminating the heat transfer surface, the orientation of the illuminating source with respect to the surface and the crystal layer uniformity on the process are investigated. The techniques developed from the concepts described in this chapter are frequently employed in studies described in Chapters III, IV, V and VI.

List of Symbols

c	=	specific heat
CCD	=	charge coupled device
CIE	=	Commission Internationale de L'Eclairage
D	=	jet exit diameter
E	=	power distribution of the illuminant
h	=	convective heat transfer coefficient $h=q/(T_{rec}-T_{wall})$
H	=	normalized hue
HSI	=	hue,saturation,intensity, (normalized)
I	=	local intensity
k	=	thermal conductivity of air
L	=	illumination length to heat transfer plate distance
m	=	slope of hue versus temperature relation
n	=	intercept of hue versus temperature relation
Nu	=	Nusselt number , $Nu=hD/k$
NTSC	=	National Television System Committee
q	=	heat flux
r	=	radius
R	=	reflectance characteristic of the colored surface
RGB	=	red, green, blue, (normalized)
Re	=	local Reynolds number based on jet exit diameter and centerline velocity
R35C1W	=	Chiral Nematic liquid crystal starting to respond at about 35 °C with an approximate bandwidth of 1 °C
S	=	saturation
t	=	time
T	=	temperature
TRS	=	total tristimulus value
TU	=	turbulence intensity
U,V,W =	=	three components of mean velocity
x,y,z	=	chromaticity coordinates
X,Y,Z	=	tristimulus values

Greek symbols

α	=	thermal diffusivity of air , $\alpha=k/(\rho c_p)$
β	=	non-dimensional time , $\beta=h.(t/pck)^{1/2}$

δ	=	actual saturation distance between white point and the specific color at a given hue
θ	=	illumination angle measured from the heat transfer surface
ϕ	=	hue angle measured from red-white line in degrees
ρ	=	density of air
λ	=	wavelength

Subscripts

∞	=	free stream
w	=	local wall condition
jet	=	jet centerline condition at the exit
rec	=	recovery
p	=	at constant pressure
i	=	initial
λ	=	spectral local value

II .1 Color Vision Principles for Liquid Crystal Image Interpretation

Color perception is a psychophysical phenomenon which results from the human eye's translation of radiant energy into visual stimuli. Color may be defined as the combination of those characteristics of light that produces the sensations of hue, saturation and intensity in a normal human observer. Intensity of a color refers to the relative brightness of a color. This quantity represents a total sum of the spectral energy incoming to the eye/sensor, emitted by an object at various wavelengths in the visible electromagnetic spectrum. Hue refers to that attribute of color that allows separation into groups by terms such as red, green, yellow, etc. In the visible spectrum, hue corresponds directly to the dominant wavelength of the light incoming to the sensor. Saturation refers to the degree to which a color deviates from a neutral gray of the same intensity - called pastel, vividness, etc. Saturation may also be defined as a color purity or the amount of white contained in a specific color. By mixing a main hue (e.g. red) with white at different amounts, one can always generate less saturated colors (e.g. tones of pink). The amount of saturation is directly proportional to the amount of white added.

Any color of the spectrum when highly de-saturated should approach standard white color. These three characteristics, hue, saturation and intensity represent the total information necessary to define and/or recreate a specific color stimulus. Conceptually, this definition of color is highly convenient and appropriate for an image-processing system to be used in the determination of convective heat transfer parameters from a liquid crystal sprayed surface, simply because the temperature of the point of interest is directly related to the hue value of the

color displayed at that point. Since the relative orientation of the liquid crystal is the main controlling parameter for the color (hue, wavelength), a direct relation between the local temperature and the locally measured hue value can be established. The orientation of liquid crystals is altered by the local temperature distribution on the heat transfer surface. Any temperature change at a given point on the liquid crystal covered surface results in a significant change in the local spectral reflectivity of this point, and therefore a color change is sensed by human eye or a visual sensor.

Color sensation from a liquid crystal covered surface is generated by a number of characteristics such as the orientation of the crystals on the surface, the spectral characteristics of the light illuminating the liquid crystal covered surface and the spectral response of the color sensing component which may be human eye or an imaging sensor used in a color camera. To determine specific parameters that describe a color on a heat transfer surface, three highly interrelated factors must be taken into account:

- 1) *Spectral reflectivity of the surface being observed. This quantity is controlled by the liquid crystal layer, coated uniformly on the heat transfer surface.*
- 2) *Spectral distribution of the light source illuminating the heat transfer surface.*
- 3) *Spectral sensitivity of the imaging sensor.*

Most of the available present day imaging sensors such as color CCD arrays simulate the spectral sensitivity of the standard human eye. The main task of the presently developed image-processing system hardware and algorithms is to bridge the perceived quantitative color information and the local temperature at a given point on a liquid crystal covered surface for heat transfer research purposes. The method assumes that perceived color changes due to slight changes in the illumination characteristics can be minimized and calibrated. The spectral response of the imaging sensor can also be taken into account during a typical hue versus temperature calibration procedure, developed during the present study.

A color vision system uses a number of principles derived from a mathematical color matching model established by Grassman as described in Wyszecki and Stiles (1967) and Pritchard (1977). The basic principles used in modern tristimulus colorimetry are as follows:

- 1) *The human eye can distinguish only three kinds of differences, which we now call hue (dominant wavelength), saturation and intensity.*
- 2) *In a two component color mixture if one component is held constant and the other changed gradually, the color of the mixture will change gradually.*
- 3) *Lights of the same color (same dominant wavelength, saturation and intensity)*

- will produce identical effects in mixtures regardless of their spectral distribution.
- 4) The intensity produced by a mixture of several lights is equal to the sum of the intensities of the individual lights.

According to the tri-receptor theory of vision, the human eye translates radiant energy to visual stimuli by using three sets of cones and rods having individual response curves in the red, green and blue portions of the visible spectrum as shown in figure 2.1. The human eye detector evaluates the intensity of an image by summing the stimuli from the three receptors, while the chromatic attributes, hue and saturation are determined by the ratios of the stimuli. Thus, light sources having widely different spectral distribution may give exactly the same visual color sensation as long as the amount and ratios of the total stimulation are the same. The intensity obtained by summing the stimuli from the three receptors is represented by a luminosity function. The details of the definitions are described by Bingley (1953), Fink (1955), McIlwain and Dean (1956), Overheim and Wagner (1982) and Pearson (1975).

The basic principles and analysis given in these references state that only three independent quantities are required to specify a color and that color intensities add linearly. Therefore, a color specification system can be envisioned as involving a three-dimensional color space with any set of convenient coordinates, and these coordinates may be transformed mathematically into any other set for convenient measurement or analysis. Colorimetric coordinate systems which can be used include the intensities of three color primaries R , G , B or hue, saturation and intensity H , S , I , or intensity and two color difference signals (I , $R-I$, $B-I$). The fundamental quantities of tristimulus colorimetry as established by the Commission Internationale de L'Eclairage (CIE) are as follows;

(2.1)

X , Y and Z are the definitions of tristimulus values and the integrations are taken through the visible region of the spectrum. E_λ represents the spectral power distribution of the illuminant in which the coloured object is viewed. The function R_λ represents the reflectance characteristic of the coloured surface, that is, the proportion of incident light which is reflected, expressed as a function of wavelength. This quantity is strictly controlled by the liquid crystal as a response to local temperature. The three functions x , y and z describe the standard psychophysical characteristics of a normal human eye as shown in figure 2.2. Using the tristimulus values as fundamentals, other related quantities called “chromaticity coordinates” may be defined, as follows;

(2.2)

The quantity $TRS = (X + Y + Z)$ is called the total tristimulus value. It may be written that;

(2.3)

The tristimulus values express the psychophysical assessment of a color by a standard observer whose characteristics have been established by a number of observers. The tristimulus values can also be transformed into a two-dimensional set of values describing the chromaticity values (hue and saturation), independent of intensity. In effect, x , y and z represent the relative amounts of the three imaginary primaries required to match a particular color. Since $x + y + z = 1$, once two of the three numbers x , y , z are given, the third is automatically determined. A graphical representation of x , y coordinates are shown in figure 2.3. Every (x , y) point on this diagram represents a unique color or chromaticity. It turns out that the chromaticities for all physically possible spectra are confined to a single region of the chromaticity diagram as shown in figure 2.3. This region is called the "color locus." Chromaticities outside the color locus are impossible to achieve with any spectrum of light from the visible spectrum. The horse-shoe shaped outer boundary of the color locus represents the characteristics of all pure colors of the visible spectrum. The corresponding wavelengths are labeled around the periphery of this curve, which is also known as the spectrum locus as shown in figure 2.3. The lower portion of the locus is bounded by a straight line that connects the blue and red ends of the spectrum locus. The straight line is known as the purple line. Hues along this line are not produced by any single wavelength of light but rather, result from the mixture of red and blue light. Points along the periphery of the color locus (along the spectrum locus and purple line) represent colors of the maximum saturation. As we move towards the center of the color locus, the saturation diminishes until, at the point ($x=0.333$, $y=0.333$) the saturation becomes zero. This central

point labeled M in figure 2.3 represents equal energy white. The exact definition of white point in terms of chromaticity coordinates may vary slightly in different video standards.

The chromaticity diagrams shown in figure 2.3 can be used to analyze color mixtures or determine dominant wavelength and saturation of a color. Point N in figure 2.3 represents the chromaticity of some spectrum of light. If a line is drawn from point M through N until the line strikes the spectrum locus at point O, point O will be located at a particular wavelength on the spectrum locus, λ_D . Thus knowing λ_D gives an immediate idea of what kind of color N really is. White point M is considered to have zero saturation while a pure color such as O is considered to be 100 % saturated. Then saturation at point N expressed as a percent is given by;

$$(2.4)$$

Saturation is a purity of the color, or how far it is removed from white toward the full color of the spectrum locus. Intensity I is most of the time specified separately from hue and saturation. For some spectra, the chromaticity may lie at a line which strikes the purple line rather than the spectrum locus. Saturation can still be calculated as described previously. For the hue (dominant wavelength) calculation, it is only needed to extend line MP backwards until the line hits the spectrum locus. The wavelength at which this occurs is called complementary dominant wavelength λ_{CD} of the color P. Further details of RGB and HSI domain color operations are given in Kender (1976), Ohta et al. (1980) and Pratt (1978).

II . 2 The Present Hue Capturing System

There are three primary color systems which have different color standards. Those are NTSC (National Television System Committee), PAL (Phase Alternation Line) and SECAM (Sequentiel Couleur Avec Mémoire). The present real time hue-capturing system operates using an NTSC standard 24 bit color image-processing system. The system is capable of converting RGB information into HSI on each of the pixels in a 512 x 512 image, using a real time electronic hue converter.

The locus of the colors reproducible by three color primaries (R,G,B) of NTSC and PAL/SECAM are shown in figure 2.4. According to Pritchard (1977), the three color primaries have been purposely changed to obtain higher picture brightness values even though colorimetric errors are introduced. The boundary of all available colors from discrete color points, pigments, films and dye processes are also compared with respect to the NTSC and PAL/SECAM color boundaries. The exact definitions of NTSC pure colors are red ($x=0.67$, $y=0.33$), green ($x=0.21$, $y=0.71$) and blue ($x=0.14$, $y=0.08$). The white point is defined as ($x=0.310$, $y=0.316$). The spectral distribution of the liquid crystal color display is converted into the attributes of three color primaries (R, G, B) using the standard filters of color video camera. The imaging device used in this study has a high light sensitivity color CCD sensor

consisting of about 632,000 pixels capable of generating red, green and blue attributes of 30 complete frames in a second. Red, green and blue attributes are then multiplexed and sent to the image-capturing board manufactured by Data Translation. The current system has the capability of either recording the image on a standard magnetic video tape or transferring the image data directly to the random access memory of the computer.

The current computer and the image processor can transfer a complete color image captured in real time on to a hard disk approximately every two seconds. The present color image-capturing board shown in figure 2.5 may either accept three individual R,G,B signals generated by a color camera or a multiplexed NTSC standard video signal. Three 8 bit video A/D converters generate digital signals before they are converted into a H,S,I signal for each pixel. The RGB-HSI conversion is performed on high performance electronic circuitry in real time. The absolute value of the hue assigned to each color is strictly controlled by the calibration of the RGB to HSI analog conversion unit. Standard video calibration sources are needed to calibrate the color image-capturing device. However, the calibration of the image-capturing device is transparent to the heat transfer researcher, if adjustments are not altered in the middle of a research program. Four individual frame buffers each having 512 x 512 x 8 bits of video memory is used for storing intensity, saturation, hue and additional graphics and text information. There is also a second HSI-RGB converter at the output of the four frame buffers. This section provides a real time display of the contents of the buffers on typical RGB or NTSC color monitors. The buffer contents may be captured whenever needed and the storage process can be initiated by transferring the video image to the random access memory of the computer.

The RGB triangle used by the current system and the relation between HSI and RGB color coordinates is shown in figure 2.6. By knowing the red, green, blue attributes inside the RGB triangle, one can always geometrically generate the attributes of hue, saturation and intensity. The intensity attribute is dependent on the sum of the R, G and B attributes. The chrominance attributes hue and saturation are based on the relative proportions of R, G and B. Thus the relationships of red, green and blue to the hue or saturation are highly nonlinear. A three-dimensional view of the HSI triangular model is also shown in figure 2.6. The intensity axis is perpendicular through the center of the RGB triangle. The present system uses three 8 bit video A/D converters, therefore each one of the R,G,B signals varies between 0 and 255. When they are converted into HSI values the new values are also normalized in such a way that they remain between 0 and 255.

The definition of intensity is as follows;

$$(2.5)$$

Saturation is defined as δ/l for the local point N as shown in figure 2.6. The lines connecting the R, G and B points of the triangle carry the maximum available saturation of a given hue.

Any movement from the maximum saturation line to the center of the HSI triangle makes this specific hue more de-saturated. The point at the center of the triangle represent the color white. The saturation values around the periphery of the triangle are at a maximum value of 255. The hue is modeled as the angle ϕ rotating around the intensity axis with 0 at R, 120 at G, and 240 at B. In dimensionless form, hue may be expressed as $\phi/360$ for the point N. The normalized expressions of the saturation and hue values in 8 bit integer scale are as follows;

$$(2.6)$$

$$(2.7)$$

The δ/l and $\phi/360$ can be calculated from the R,G,B attributes. The model resulting from the following expressions is based on an equal sided triangle with the white point located exactly on the center of gravity of the triangle. The conversions from R,G,B attributes are as follows;

$$(2.8)$$

$$(2.9)$$

Further details of this approach are described in Berns (1989).

II . 3 The Model for Hue versus Temperature Calibrations

In order to validate the current hue-capturing technique on a liquid crystal covered heat transfer surface, a 19.7 mm thick flat plexiglass plate was manufactured. The plate had a total surface area of 1.0 x 1.0 m². One side of the plexiglass plate was coated with a micro-encapsulated chiral nematic liquid crystal layer (R35C1W) purchased from Hallcrest Inc. After the application of the crystal layer on the plexiglass flow side, a black coating was applied on top of the temperature sensitive liquid crystal layer as shown in figure 2.7. The top surface of the model was designated as heat transfer surface. Convective heat flux was always applied from the top surface. However, the imaging camera was located at the bottom of the plexiglass model. This approach provided a viewing angle which was normal to the heat transfer surface.

The illumination system was also located on the camera side of the plate. The model was carefully covered in order not to damage the crystals from exposure to ultraviolet light. A direct exposure of the liquid crystal surface to sun light was avoided. It was also expected that most of the ultraviolet light was going to be filtered during passage from laboratory windows and the thick (19.7 mm) plexiglass plate.

Four fast response K-type thin foil thermocouples were flush mounted at separate locations on the heat transfer model for calibration purposes. The thermocouples had typical time response of about 2 milliseconds. The temperature measurement chain was carefully calibrated. The uncertainty of the temperature measurement with the thin foil thermocouple was expected to be within ± 0.15 °C. Temperature recording was performed by using a 4 and 1/2 digit temperature readout made up of red 7 segment light emitting diodes. The readout was located on the camera side of the heat transfer plate. The video recordings of the liquid crystal image also carried the instantaneous temperature information at a local point. The time response of the whole temperature measurement chain was of the order of 100 Hz. This response guaranteed a correct temperature recording on each of the sequentially captured images, captured at a standard rate of 30 frames per second.

II . 4 Hue Calibration Results and Discussion

II.4.1 Hue versus Temperature Relation : A baseline experiment was performed on the liquid crystal coated surface in order to find out the dependency of the liquid crystal color to temperature. The local temperature of the liquid crystal surface was changed by applying a radiative heat flux from a temperature controlled heated plate. An extremely slow varying color pattern and the thermocouple temperature readout were recorded simultaneously. Two sets of color defining parameters including (R, G, B) and (H, S, I) at the thermocouple location were obtained at different local temperatures as shown in figure 2.8. Temperature smaller than 35.3 °C is a region out of the liquid crystal color response band. Liquid crystal shows “almost black” color in this region. The term “almost black” was used here because any pure color may appear “almost black” under low intensity condition. The hue distribution for this specific experiment provide a continuous color spectrum from red, yellow, green and finally to blue for the temperature between 35.3 °C and 37.0 °C. The hue values ranged from 0 to 170 for the temperature range. The corresponding intensity values varied between 60 and 170. The peak intensity point corresponded to the temperature at which a green color appeared, around a hue value of 90. The saturation values do not show any interesting features for the variation of temperature. This is due to the fact that local temperature correlates only with the wavelength of the color from a liquid crystal image, not with the amount of white contained in the specific color. The peaks of red, green and blue attributes appeared at 35.6, 35.8 and 36.2 °C, respectively. Liquid crystal surface shows blue color for a while beyond 37.0 °C and finally becomes “almost black “ again.

Figure 2.9 shows the details of hue versus temperature relation. The color information in the form of hue shows a very linear variation with respect to local temperature between 35.3 °C and 36.3 °C. The hue values smaller than 30 represented the “almost black” zone appearing just before red for the specific liquid crystal used, (R35C1W). The hue range between 30 and 140 contained typical colors such as red, orange, yellow, green and blue. This linear range was the most useful part of the hue versus temperature relation in terms of performing accurate temperature measurements using the color-capturing technique. A complete spectrum of colors was located in an almost 1 °C wide temperature band. The discrete data points shown in figure 2.9 showed an uncertainty band of less than ± 0.1 °C in the hue range between 30 and 140. However, this uncertainty band was obtained only from data scatter of the hue versus temperature relation. The final uncertainty band of the technique was estimated to be ± 0.25 °C, since the calibration was performed with a thin foil thermocouple having an uncertainty band of ± 0.15 °C. The hue values above 140 corresponded to the wide dark blue zone which is very typical of liquid crystal images. The present color image-processing system uses an eight bit discretization for the hue-capturing process. This feature allowed division of the complete color range into 256 units. For the specific liquid crystal calibrated (R35C1W), the slope of the useful hue range suggested that a 0.92 °C change in the local temperature corresponded to a relative hue change of 100 hue units.

II.4.2 Effect of Illumination Source on Hue versus Temperature Calibration : It is a known fact that color perception from a liquid crystal image is influenced by the type of the liquid crystal applied, the amount of light illuminating the surface, spectral response of the color image sensing device, uniformity of the sprayed liquid crystal layer, in addition to the selective reflectivity of the surface which is controlled by the liquid crystal in function of the local temperature. The effect of the amount of the light illuminating the heat transfer surface on color-capturing process is given in figure 2.10a. An incandescent light source (500 W, 3200° K) contained in a reflector was used to illuminate the liquid crystal applied surface. The light source was kept at $\theta = 40^\circ$ to the surface for all of the experiments, unless otherwise stated. All of the experiments were performed during the night in complete darkness in order to eliminate the contribution of all other light sources, except the illuminating source.

Figure 2.10a compares the results from five different experiments each with a different light source to model distance with the same source. The distances were varied from 1.25 to 1.50, 1.75, 2.00 and 2.25 m. The figure shows that the change in captured hue values due to the varying amounts of illuminating light intensity was not very significant. When all of the points were compared, the uncertainty introduced by the light source distance variations was well within ± 0.1 °C.

Figure 2.10b shows the influence of illumination angle on hue measurements. For the experimental results shown in this figure, the light source to model distance was always kept constant at 1.75 m. The illumination angle was measured from the flat heat transfer surface. At

small angles ($\theta = 20^\circ, 30^\circ$ and 40°), the influence of the illumination angle was negligible as far as the linearity of the hue-temperature relation was concerned. However, after $\theta = 40^\circ$, the deviation from the linear part of the hue versus temperature line became increasingly larger. At $\theta = 60^\circ$, the temperature uncertainty increased to values as large as $\pm 0.2^\circ\text{C}$, especially for the temperature range above 36.0°C . The range below 35.0°C was not significantly influenced by the illumination angle variations.

Figures 2.10a and 2.10b suggest that the color-capturing process on a liquid crystal covered surface should be performed always with the same illuminating source, the same light distance and the same illumination angle. The distance and the angle of the light source should be kept the same both for the calibration and the actual experiment, for a more accurate temperature measurement.

The camera conditions such as imaging sensor (circuit) gain, filter adjustment, diaphragm aperture, optical adjustments (zoom, etc.) should also be kept unchanged for all of the tests including the hue versus temperature calibration process. The image-processing system color-capturing adjustments have to be locked during the calibration and actual testing efforts.

II.4.3 Spatial Distribution and Repeatability of Liquid Crystal Color Response: The microencapsulated Chiral-Nematic liquid crystal and the binder mixture was sprayed by using a pressurized air brush as uniformly as possible. In order to check the spatial uniformity of the color response, three individual thin foil thermocouples were flush mounted at separate locations on the flat heat transfer surface. The hue versus temperature calibrations were repeated at each location individually using a number of local temperature levels. The results are presented in figure 2.11a. The comparison of hue versus temperature curves at the three locations indicated that the liquid crystal color response provided a very consistent and reliable temperature measurement. The uncertainty band for the uniformity confirming experiments was better than $\pm 0.1^\circ\text{C}$. Figure 2.11b presents the repeatability tests performed on three separate days at the same thermocouple location. The thin foil thermocouple located at the center of the plate was used for these tests. The exact same calibration procedure resulted in highly repeatable calibration curves as shown in figure 2.11b. The maximum repeatability error was easily within $\pm 0.1^\circ\text{C}$ in the linear portion of the hue versus temperature curve.

II.4.4 Hue versus Intensity: The present color image-processing technique provided simultaneous hue, saturation and intensity values at each pixel location in real time. A very linear, reliable and repeatable hue-temperature relation is shown in figure 2.9. The experiments in the present program showed that, intensity information may also be used in processing liquid crystal data for quantitative heat transfer measurements. Figure 2.11 shows a high resolution hue versus temperature relation from a few hundred discrete hue-temperature measurements using the present digital image-processing system. A slowly varying temperature pattern on the

thermocouple location was recorded on a video tape with its complete color image at a rate 30 frames per second. The image also consisted of the real time seven segment LED display indicating the instantaneous thermocouple measurement. The details of the simultaneous hue and intensity measurements for a liquid crystal with a color play temperature of 42.8°C are given in figures 2.12, 2.13 and 2.14. The total bandwidth of the Chiral Nematic liquid crystal was approximately 1.0°C , (R42C1W) as specified by the manufacturer..

The experiments performed with a high temperature resolution showed that, there was always a very distinct intensity peak in the intensity versus temperature variation as presented in figure 2.13. The peak appeared at 43.05°C , corresponding to a very narrow color band was mainly dominated by green. A close examination of figures 2.12 and 2.13 showed that the local temperature corresponding to the intensity peak may easily be determined. Figure 2.13 suggested that a single isotherm could be captured in a very accurate manner by carefully determining the peak intensity levels from a given image. For example, in an actual test under the same illumination conditions, the locus of intensity peak points may be associated with the isothermal line of 43.05°C occurring at a hue level of 107 hue units.

Cross plotting hue and intensity is a very useful tool in setting up the illuminating system for a successful heat transfer experiment with well defined hue points. It is a known fact that color image sensors do not respond in a healthy manner when the local intensity level or saturation is below a certain value. The illumination system should be adjusted in such a way that a typical hue distribution is obtained at reasonably high local intensity levels. Figure 2.14 shows a hue-intensity cross plot at the location of the calibration thermocouple. All of the colors locally appearing from red to blue located themselves between a hue level of 0 and 170, on a slightly curved line. Figure 2.12 correspondingly showed that the hue levels above 140 are out of the linear portion of the calibration curve for the specific liquid crystal used (R42C1W). Above a hue value of 140, the captured data points remained in the dark blue-black zone of the liquid crystal.

Figure 2.14 indicated an overall intensity pattern smoothly varying in a range between 50 and 100. The experiments showed that the present hue-capturing process worked very efficiently in an overall intensity range between 50 and 200. The hue versus intensity curve may be easily shifted to the right hand side of the intensity scale (figure 2.14) by simply increasing the strength of the illuminating light source. It was found that the intensity levels above 200 affected the hue-capturing method in a detrimental manner due to the saturation of the CCD sensor. It is also well known that very low overall illumination levels (e.g. intensity levels less than 50) makes the hue-capturing process unstable. Construction of a hue versus intensity chart using the intended illumination configuration (distance, angle, light source strength) provides a valuable and crucial check before the execution of an actual experimental program. Overall intensity levels between 50 and 200 (preferably between 100 and 150) were the typical levels for the hue-capturing process performed on the color image-processing system described in this study.

II.4.5 Isotherm Extraction from a Typical Liquid Crystal Image: The experimental calibration technique to convert color information into accurate temperature measurement was developed and tested at a local point having a fast response thermocouple flush mounted on the heat transfer surface. However, one of the final goals in this study was to obtain high resolution distributions of temperature and convective heat transfer coefficients on surfaces with complex geometry or characteristic lines. In order to show the further applicability of the method, a baseline experiment was designed by using a heated round jet of air, stagnating on a flat plate. The liquid crystal covered surface was heated by the heated jet originating from a round pipe as shown in figure 2.7.

The heated jet flow system will be described in detail in chapter 3. This configuration provided a steady axisymmetric temperature distribution on the plate with maximum temperature at stagnation point. A concentric coloured ring around the stagnation point was observed at specific radial locations from the point.

Figure 2.15 shows the distributions of hue, saturation and intensity of the concentric coloured image along the radius within the first two jet diameters radial distance. The circumferential uniformity of the jet flow was carefully checked and adjusted so that the information shown in figure 2.15 represented all of the circumferential positions for this non-swirling jet flow. The hue distribution provided a very wide color spectrum from red, yellow, green and finally to blue. The hue values ranged from 0 to 170 between $r/D=0.7$ and $r/D=1.2$. The corresponding intensity values in the same radial band varied between 100 and 210. The peak intensity point corresponded to the radius at which a very narrow green color appeared, around a hue value of 90. The experiment presented in figure 2.15 and many other similar experiments run by the author showed that, the intensity peak is closely related to the green color observed on the surface. The saturation values obtained at each pixel location were not very helpful in obtaining accurate heat transfer results. Saturation of a color is strongly altered by the strength and by the geometrical orientation of the illuminating system. The saturation values were almost at an overall flat level of 40 units for the pixels having a local intensity value of greater than 100. The hue distribution shown in figure 2.15 can easily be converted into accurate temperature distribution through the use of calibration curve provided in figure 2.9. The calibration showed that hue versus temperature relation was linear between hue values of 30 and 140. For the points having an r/D value greater than 1.25, hue capturing was not well defined due to the relatively low intensity values generated by the “almost black” color which was showing the coldest zone on the heat transfer surface. The “almost black” color is an indication of a region out of the liquid crystal color response band.

An experiment was designed to see the robustness of hue-capturing process under different illuminating light strengths. An incandescent light source (500 W, 3200 °K) oriented at $\theta = 40$ degrees to the surface was used to generate different illumination conditions on the same heat transfer image. The above mentioned steady state concentric color pattern was captured when the light to model distance was changed from $L=1.5$ to 1.75, 2.00, 2.25 and finally to

2.50 m. A color video image was captured and processed for intensity and hue information useful for heat transfer studies.

The data points in figure 2.16 show the variation of local intensity values under strong illumination level changes. A surface mounted thin foil thermocouple monitored the surface temperature pattern at the center of the jet. No significant variation of wall temperature was observed at different light distances. It was found that the local intensity value was shifted from a value of 200 down to 135 when the same light source was moved from $L=1.50$ m to $L=2.50$ m, in figure 2.16. However, the qualitative distribution of intensity remained almost the same with the same peak position.

The hue distributions corresponding to the light distance experiments given in figure 2.16 are shown in figure 2.17. An excellent feature of Chiral Nematic liquid crystals of the encapsulated type was observed. Very strong local intensity variations created by moving the light source did not alter strongly the main color defining parameter "hue". This feature was expected because of the definition of the quantity "hue". Hue is a direct measure of the dominant wavelength at which the electromagnetic light emission from the heat transfer surface occurs. For the same light source located at several other distances, the only parameter that varies is the amount of total energy incoming to the surface as electromagnetic energy. The variations of the incoming total electromagnetic energy results in strong variations in the amount of reflected light from the liquid crystal covered surface. However, the spectral character of the illuminating light source was always the same for all of the experiments performed in this study. Therefore, it was expected that the spectral character of the reflected light from the heat transfer surface was not going to change if the surface temperature pattern was not altered by external means. A number of surface temperature checks also showed that thermal radiation contribution to the surface temperature pattern from the light source was quite negligible for all of the experiments presented in figure 2.17.

The maximum local temperature variation at the center of the jet was within $\pm 0.10^\circ\text{C}$ for all of the cases with different distances. It was concluded that by significantly changing the intensity of illuminating light, the local hue values did not vary in a strong manner. All of the measured hue points obtained at five separate light distances were within a hue band of ± 10 hue units. The corresponding temperature band was calculated as $\pm 0.09^\circ\text{C}$ using the relation in figure 2.9. There are a few scattered data points with unexpected magnitudes, located at the extreme edges of the stagnation area on the surface. They were attributed to color-capturing deficiencies of both the camera sensor and the RGB-HSI analog conversion process at very low local intensity levels, corresponding to "almost black" regions, ($r/D > 1.25$). From a signal processing point of view, these are highly noisy parts of a typical liquid crystal image. The very slight variation in local hue values may include some thermal radiation effects due to varying distance or shape factors. In practice, model to light distance is most of the time unchanged from experiment to experiment. If one always uses the same illuminating source at the same angular position and distance for both the calibration process and actual experiments, very accurate quantitative measurements of local temperature may be obtained as shown in figures 2.10 and

2.11.

The present color images from the stagnating heated jet experiment were sampled with a pixel resolution of 512 x 512, resulting in large data files containing 778 KBytes of digital information. At this resolution, in the useful (linear hue versus temperature) portion of the image, the temperature measurement resolution is much higher than the measurement techniques utilizing discrete point sensors, such as thermocouples, resistance thermometers, thermistors, etc. A computerized process was shown to be very effective in extracting many distinct isothermal lines or very narrow temperature bands from a color image file. Figure 2.18 shows three hue bands each having a bandwidth of 10 hue units for the same condition. Cross symbols denote the hue values between 50 and 60 which corresponded to a temperature band of 0.09°C starting from 35.49°C ($H = 50$). While solid circular symbols represent a temperature band $35.86\text{--}35.95^{\circ}\text{C}$. Plus symbols show the maximum measurable temperature range which indicates a temperature band of 0.09°C with a starting temperature of 36.23°C . The corresponding hue band is between 130 and 140. Three distinct temperature bands are located between 35.49 and 36.32°C . This kind of contouring was performed in a very time effective manner. A three-level contouring required a total of 27 seconds on the specific image processor described in this study.

II . 5 Conclusions

A color recognition method based on a real time hue capturing technique was developed for the quantitative interpretation of liquid crystal images obtained as surface thermographic records. Quantitative color perception using a hue-saturation-intensity based description was proven to result in excellent surface temperature contouring on liquid crystal coated surfaces.

It was shown that the local color play of the liquid crystal could be documented using local hue which was a direct measure of the wavelength of the light selectively reflected from the liquid crystal surface. Since the selective reflection process was controlled by the liquid crystal as a natural response to local temperature, a hue versus temperature calibration was possible. A highly linear hue versus temperature relationship was established by performing at least a few hundred local quantitative color-temperature measurements on the liquid crystal coated heat transfer surface.

The present technique allows the researcher to use many of the visible colors appearing on the liquid crystal coated surface in contrast to many previous methods only utilizing a very narrow, distinct color band which is interpreted as an iso-thermal line. It was concluded that the data density in a typical heat transfer coefficient distribution could be improved about 40 times with the present system, compared to the techniques using only a narrow color band as a single isotherm.

The influence of the illumination light strength, viewing angle, liquid crystal spatial

uniformity and camera conditions is discussed in detail.

Tests performed at the same location but at different times showed a maximum uncertainty band of $\pm 0.05^{\circ}\text{C}$ for the repeatability error.

The tests performed to plot local intensity in function of corresponding local temperature always showed an intensity peak at the location where green color appeared dominantly. The study also showed that hue versus intensity curve could be utilized in improving the hue capturing process, by quantitatively checking the overall intensity distribution on the heat transfer surface.

A powerful application of the present liquid crystal thermography method is the generation of convective heat transfer coefficients with high resolution. The pixel by pixel color capturing capability of the present method is extremely useful for two dimensional processing of color information on more complex heat transfer surfaces.

References

Berns, R. S., "Colorimetry for Electronic Imaging Devices," Tutorial Short Course Notes (T60), Center for Imaging Science/Rochester Institute of Technology, The International Society for Optical Engineering, OE/LASE '89, 1989.

Bingley, F. J., "Colorimetry in Color Television," *Proceedings of IRE*, Vol. 41, pp. 838-851, 1953.

Camci, C., Kim, K. and Hippensteele, S. A., "A New Hue Capturing Technique for the Quantitative Interpretation of Liquid Crystal Images Used in Convective Heat Transfer Studies," ASME Paper 91-GT-277, 1991, to be published in *Trans. of the ASME, J. of Turbomachinery*.

Fink, D. G. (Editor), Color Television Standards-NTSC, *McGraw-Hill*, New York, 1955.

Kender, J., "Saturation, Hue and Normalized Color: Calculation, Digitization Effects and Use," Technical Report, Department of Computer Science, Carnegie-Mellon University, 1976.

McIlwain, K. and Dean, C. E. (Editors), "Principles of Color Television," *John Wiley and Sons Inc.*, New York, 1956.

Ohta, Y., Kanade, T. and Sakai, T., "Color Information for Region Segmentation, in Computer Graphics and Image Processing", *Academic Press Inc.*, New York, 1980.

Overheim, R. and Wagner, D. L., "Light and Color," *John Wiley*, New York, 1982.

Parsley, M., "The Use of Thermochromic Liquid Crystals in Research Applications, Thermal Mapping and Non-destructive Testing," Seventh IEEE SEMI-THERM Symposium, pp. 53-58, 1991.

Pearson, D. E., "Transmission and Display of Pictorial Information," *John Wiley and Sons Inc.*,

New York, 1975.

Poinsatte and Hippensteele, "Private communication," NASA Lewis Research Center, Internal Fluid Mechanics Division, mail stop 5-11, 21000 Brookpark Road, Cleveland, Ohio 44135, USA, 1990.

Pratt, W. K., "Digital Image Processing," *Wiley-Interscience*, New York, 1978.

Pritchard, D. H., "US Color Television Fundamentals - A Review," IEEE Transactions on Consumer Electronics, Vol. CE-23, pp. 467-478, 1977.

Wyszecki, G. and Stiles, W. S., "Color Science," *John Wiley*, New York, 1967.

Zharkova, G. M., Khachaturyan, V. M., Vostokov, L. A. and Alekseev, N. M., "Study of Liquid Crystal Thermoindicators," *Advances in Liquid Crystal Research and Applications (Proceedings of the Third Liquid Crystal Conference of the Socialist Countries, Budapest, 1979)*, Vol. 2, pp. 1221-1239, 1980.

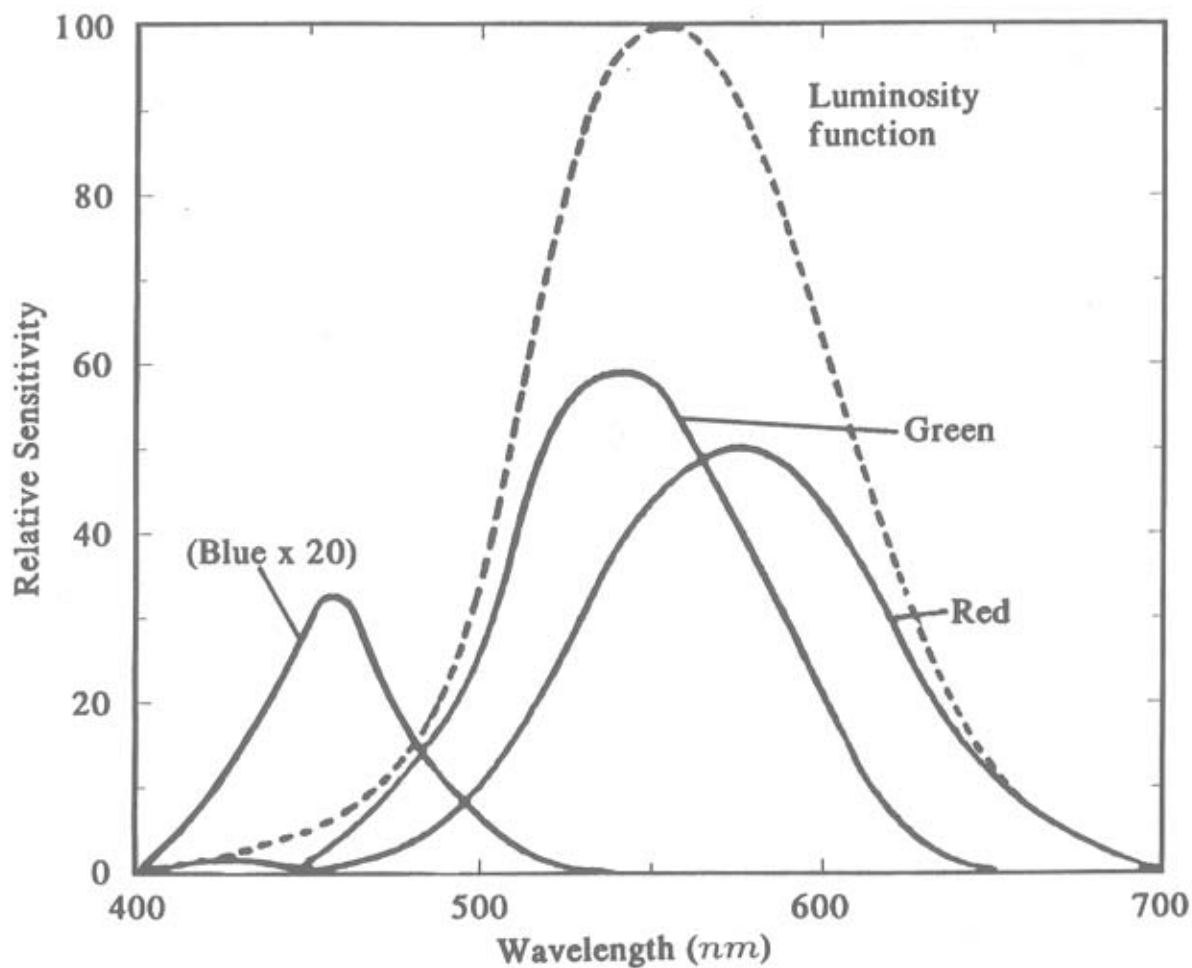


Figure 2.1 Typical human eye spectral response to light as electromagnetic radiation energy.

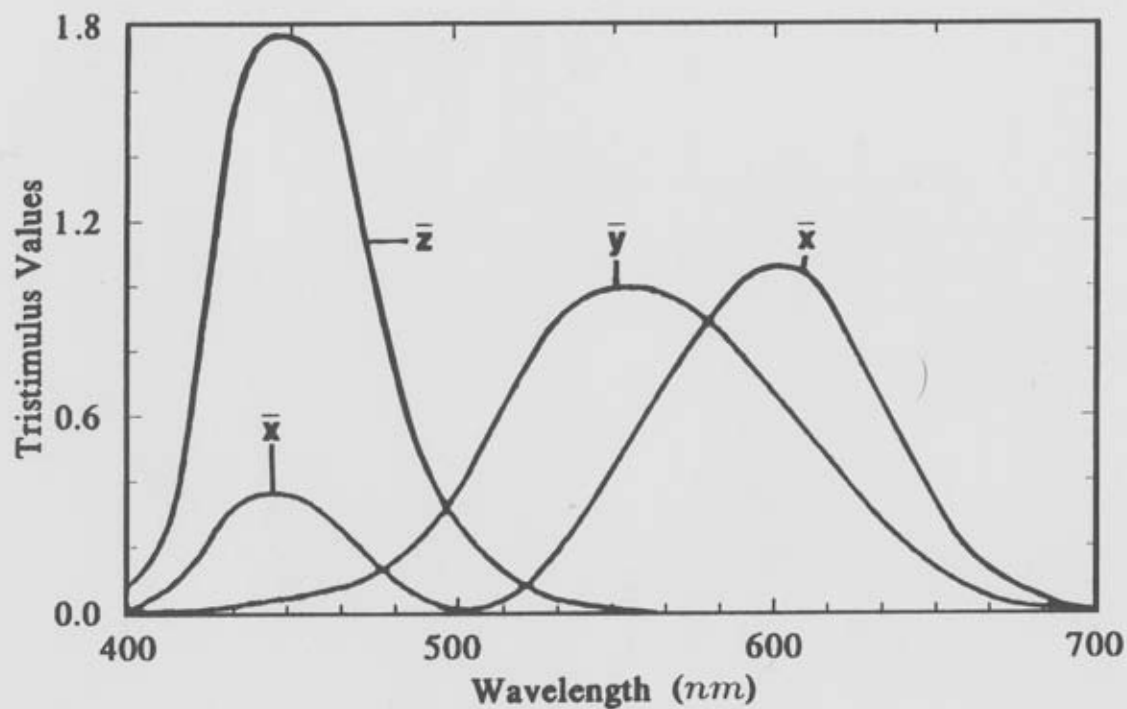


Figure 2.2 Standard psychophysical characteristics of the human eye (CIE tristimulus curves).

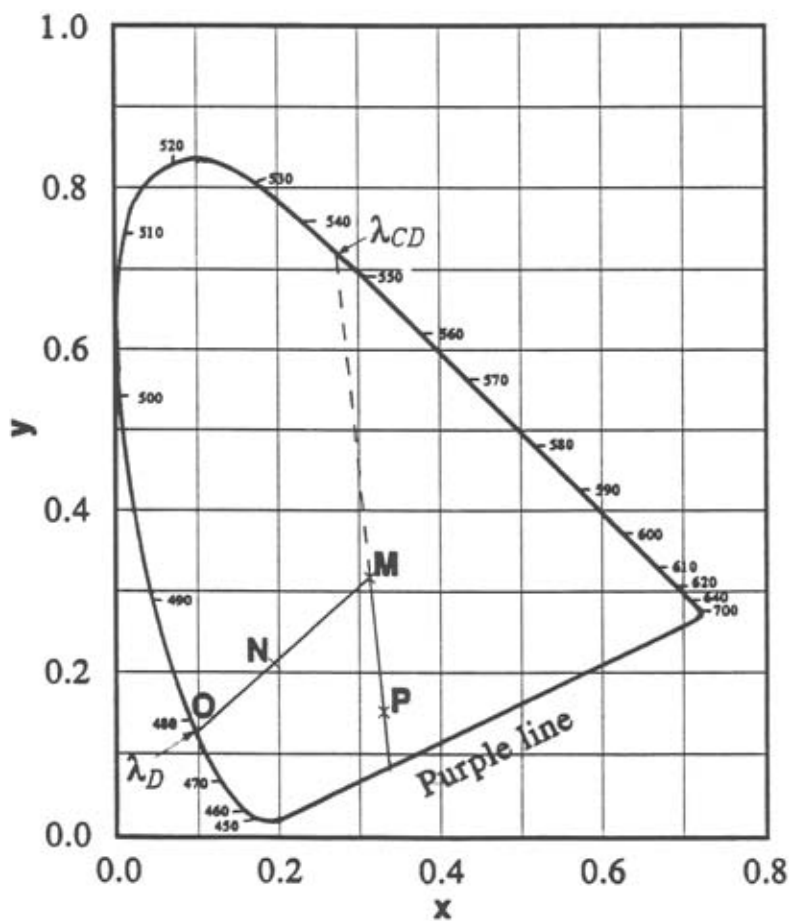


Figure 2.3 Chromaticity diagram indicating all physically possible colors from the visible spectrum.

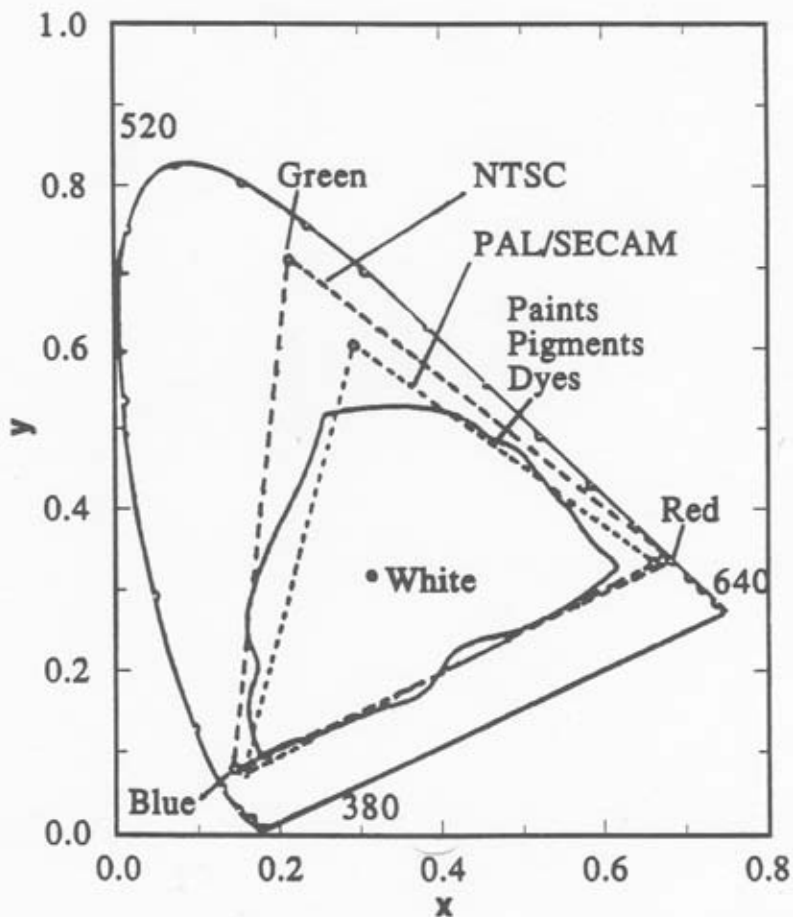
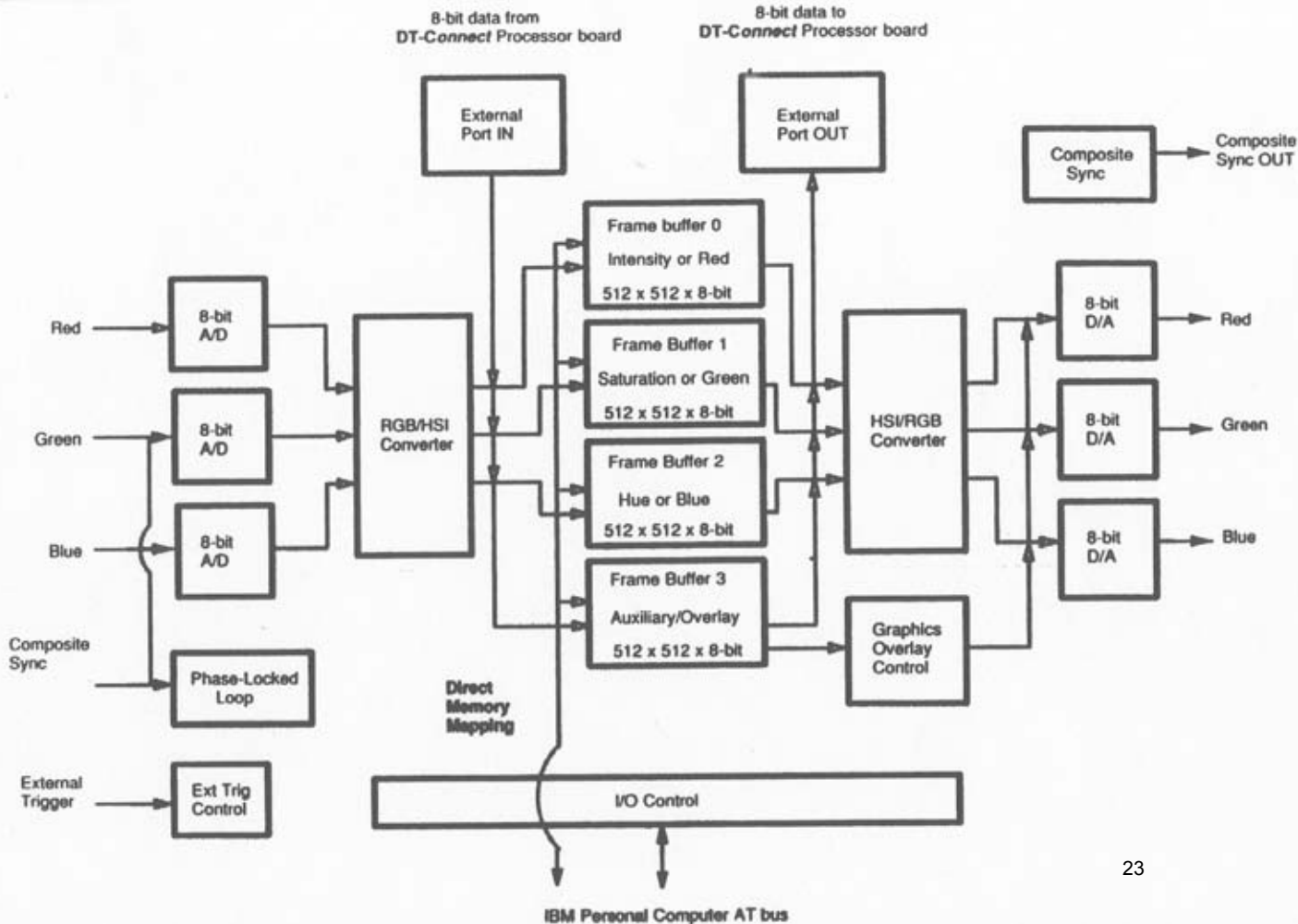
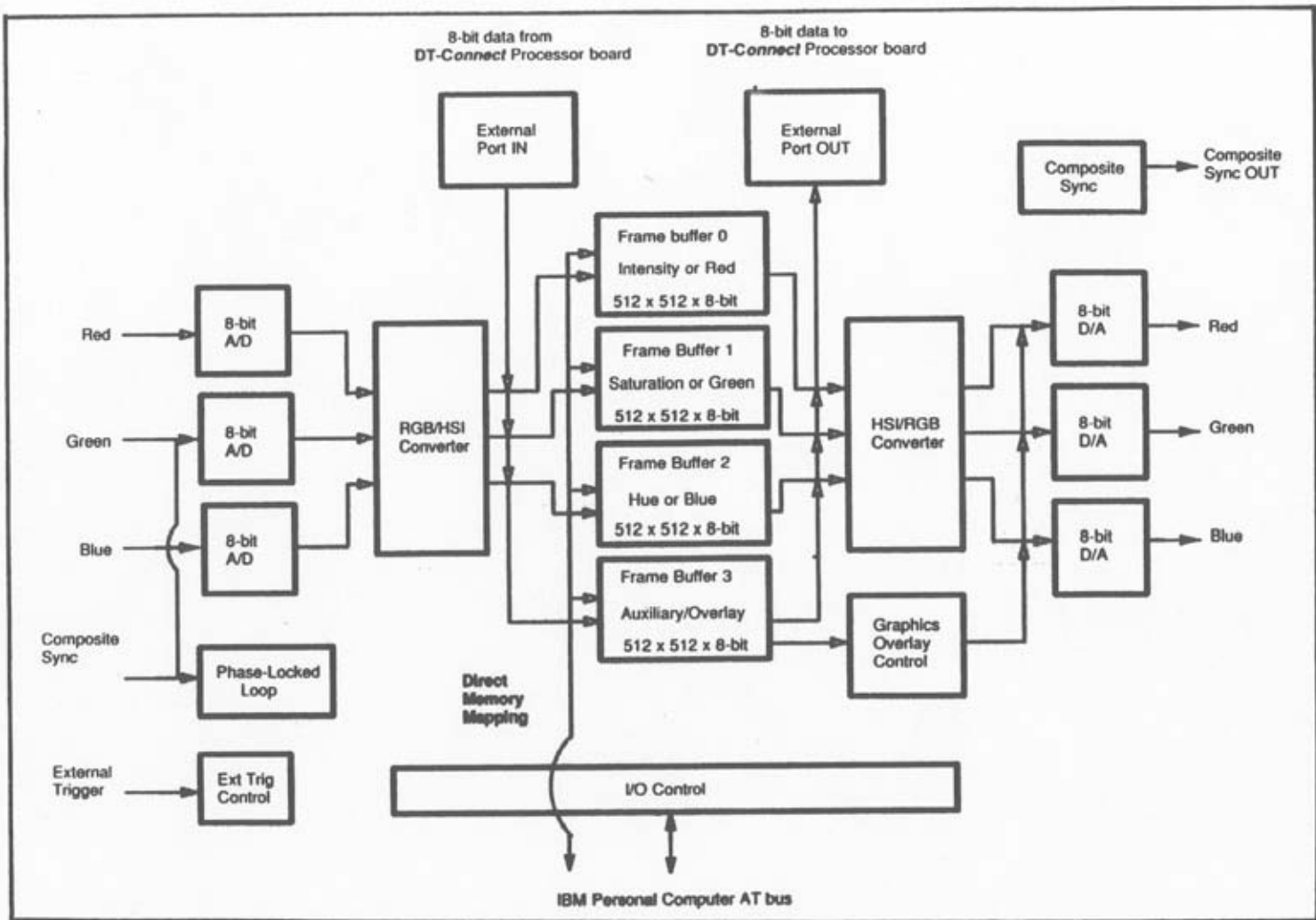
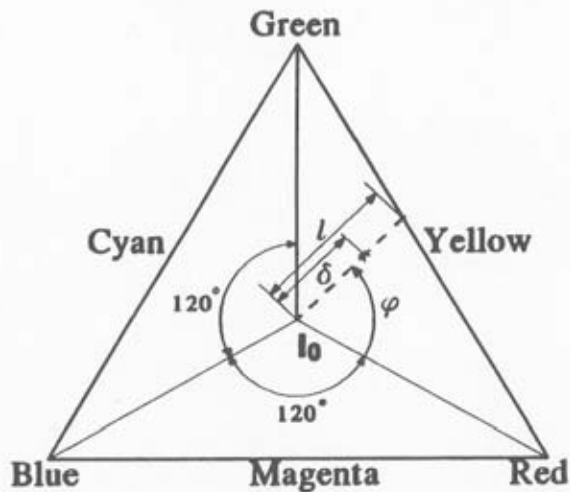


Figure 2.4 Chromaticity diagram showing all possible colors of paints, pigments, dyes including NTSC and PAL/SECAM color boundaries.





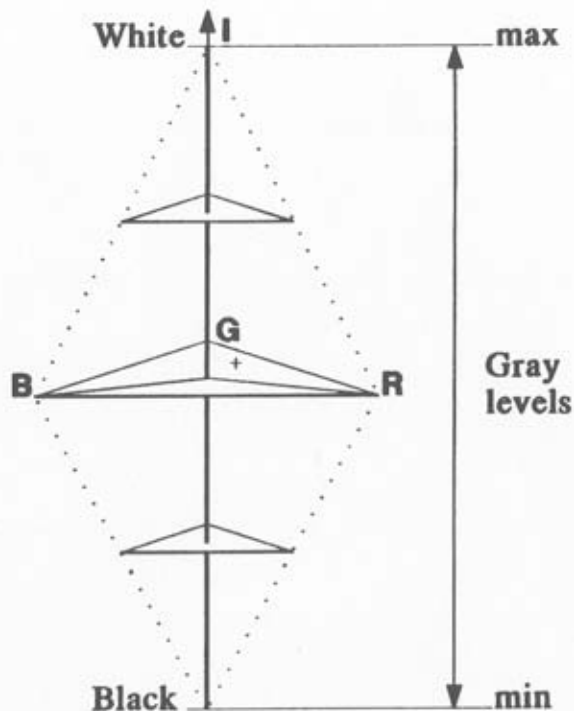
2.5 Data Translation digital image processing system.



Cross-sectional view of **HSI** triangle model
(I axis runs perpendicular to the page through I_0)

$$S = (\delta/l) * 255$$

$$H = (\varphi/360) * 255$$



3-dimensional view shows intensity axis

$$I = (R + G + B)/3$$

Figure 2.6 **RGB** triangle used by the current system, geometrical description of **H**, **S**, **I** and a three dimensional view of the present color model.

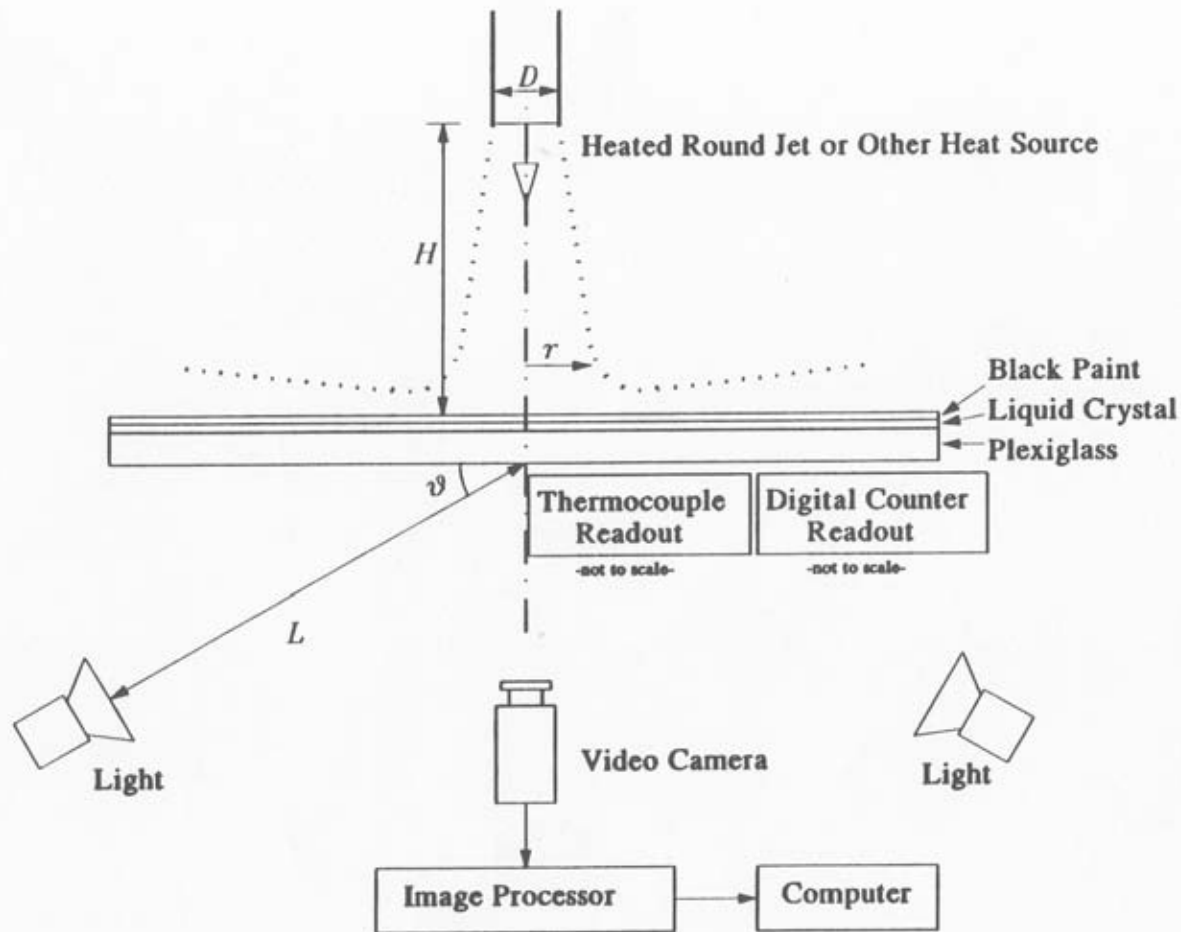
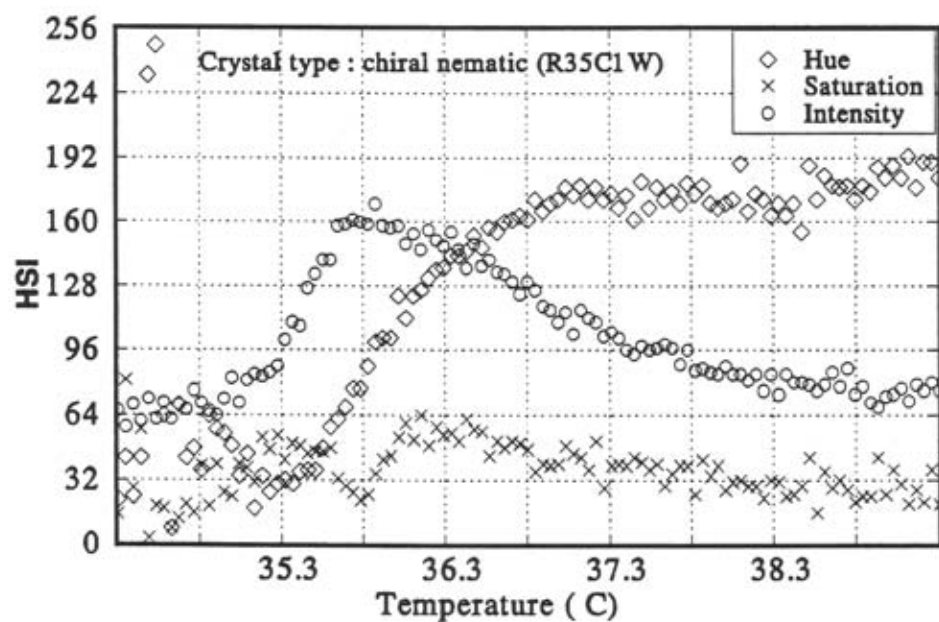


Figure 2.7 Experimental setup, the heat transfer surface and the heat source.

(a)



(b)

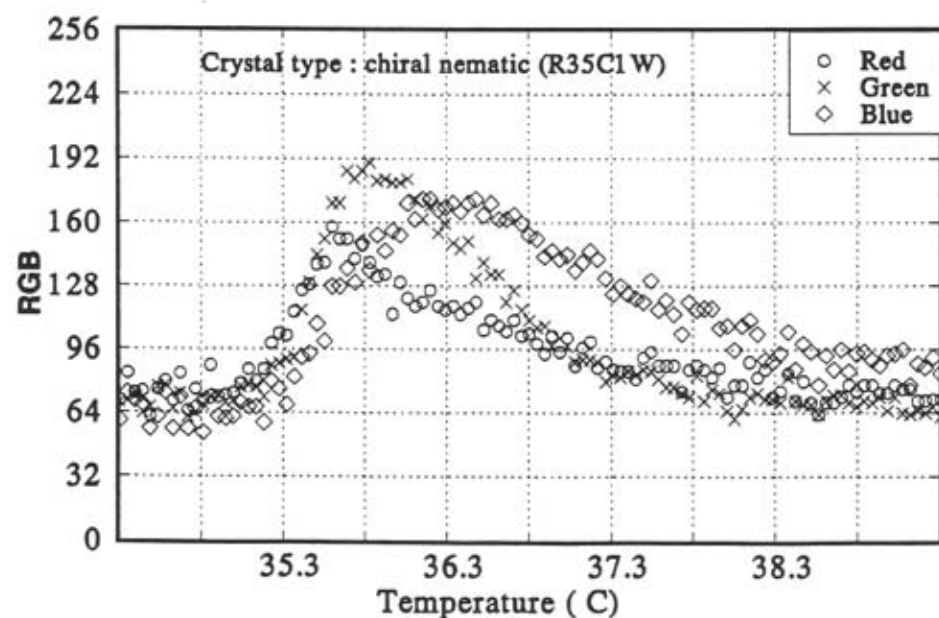


Figure 2.8 (a) HSI and (b) RGB versus temperature relations.

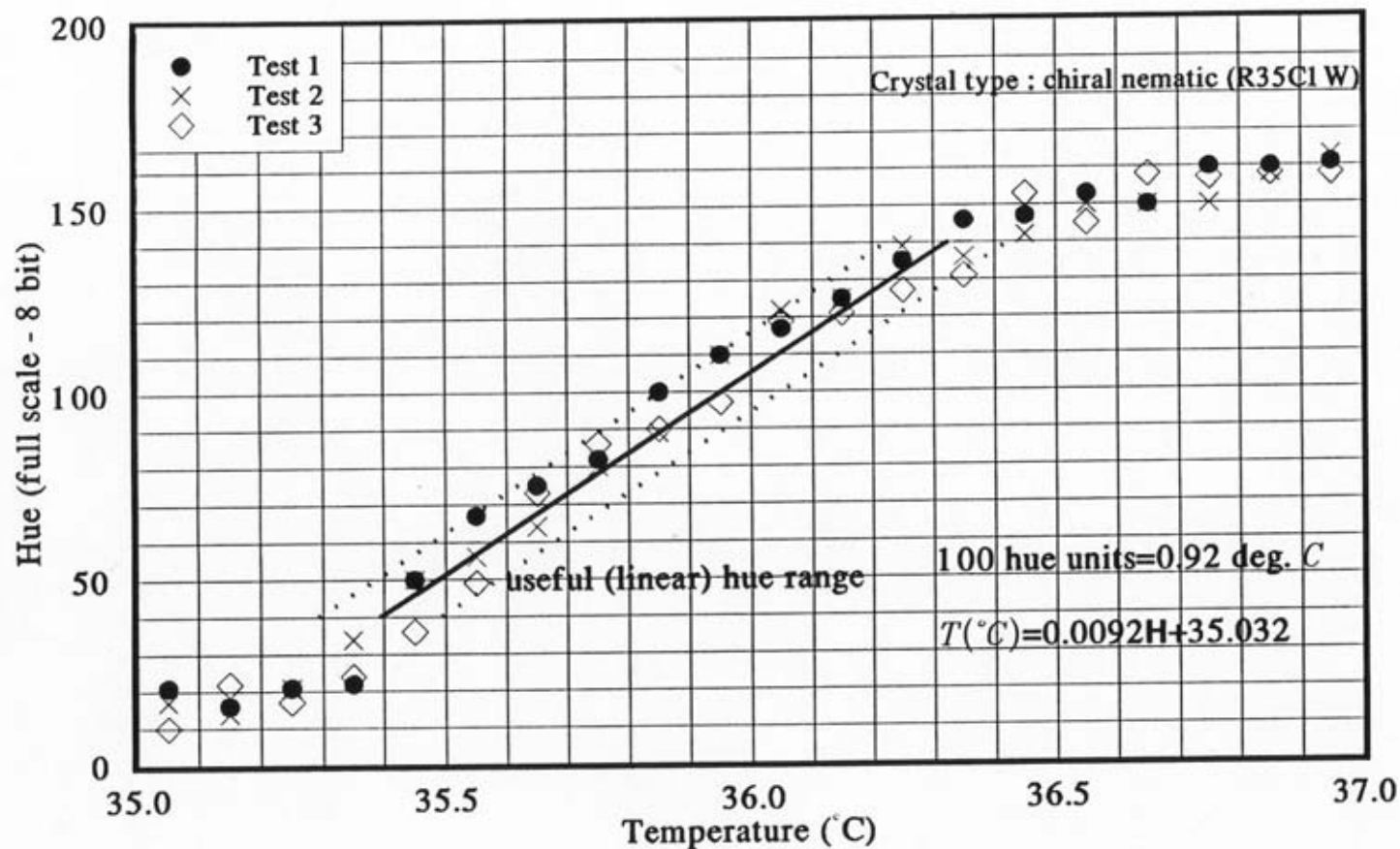
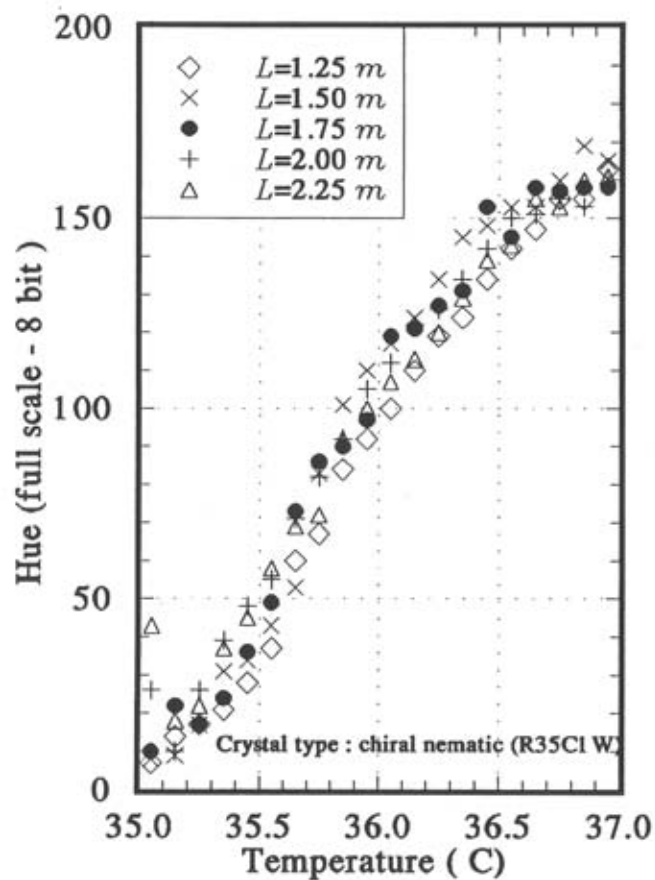


Figure 2.9 Local hue versus temperature relation.

(a)



(b)

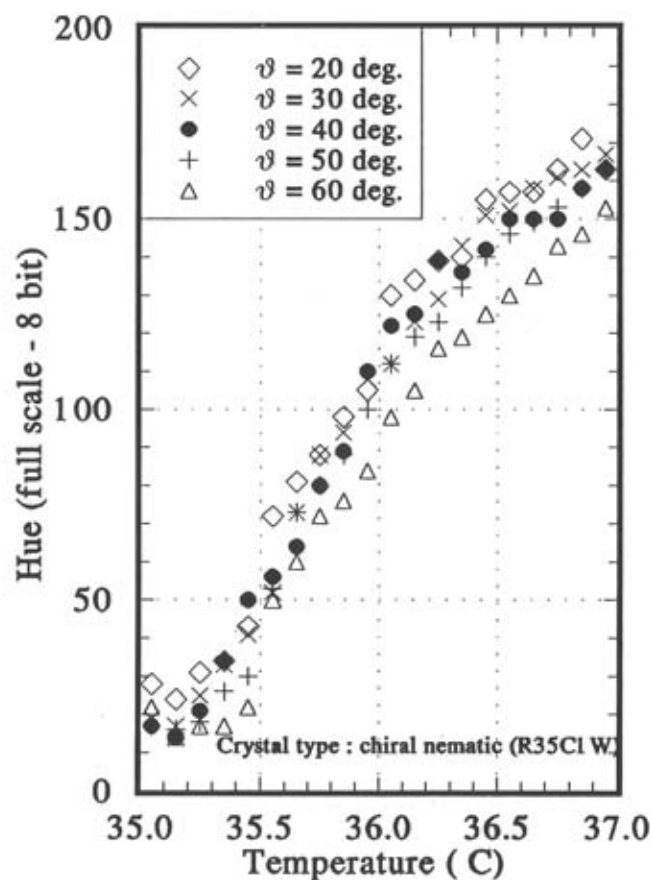


Figure 2.10 Effects of (a) light source distance and (b) illumination angle on the hue capturing process.

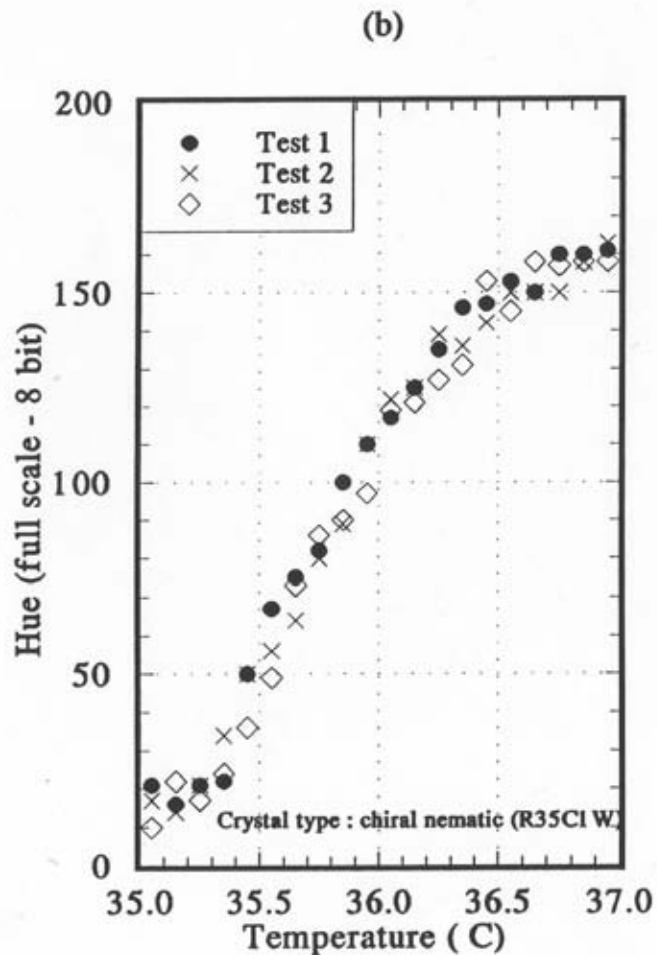
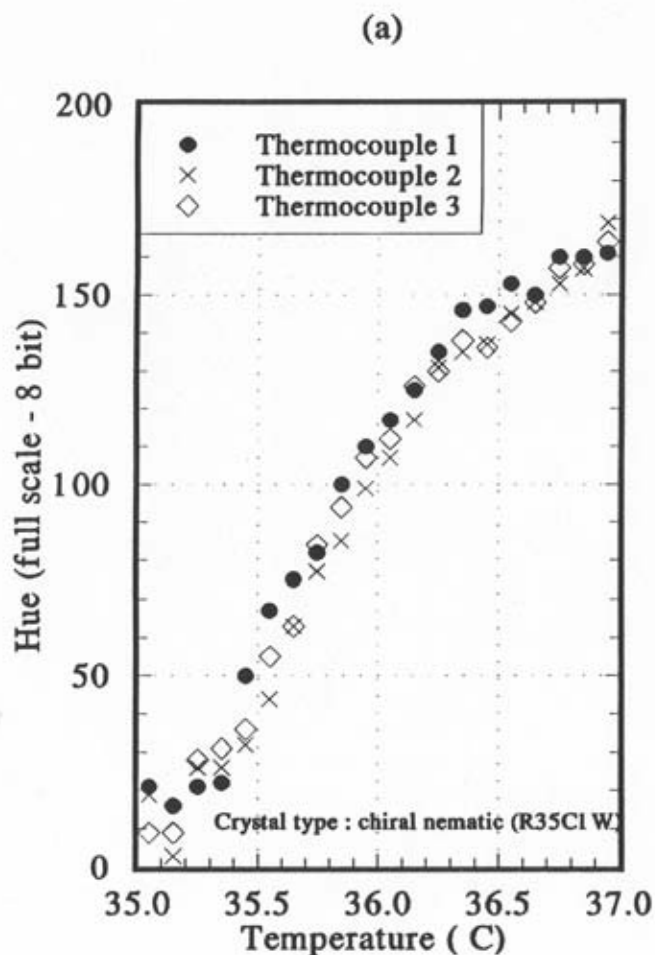


Figure 2.11 (a) Effect of liquid crystal layer uniformity on the hue capturing process and (b) repeatability of the process.

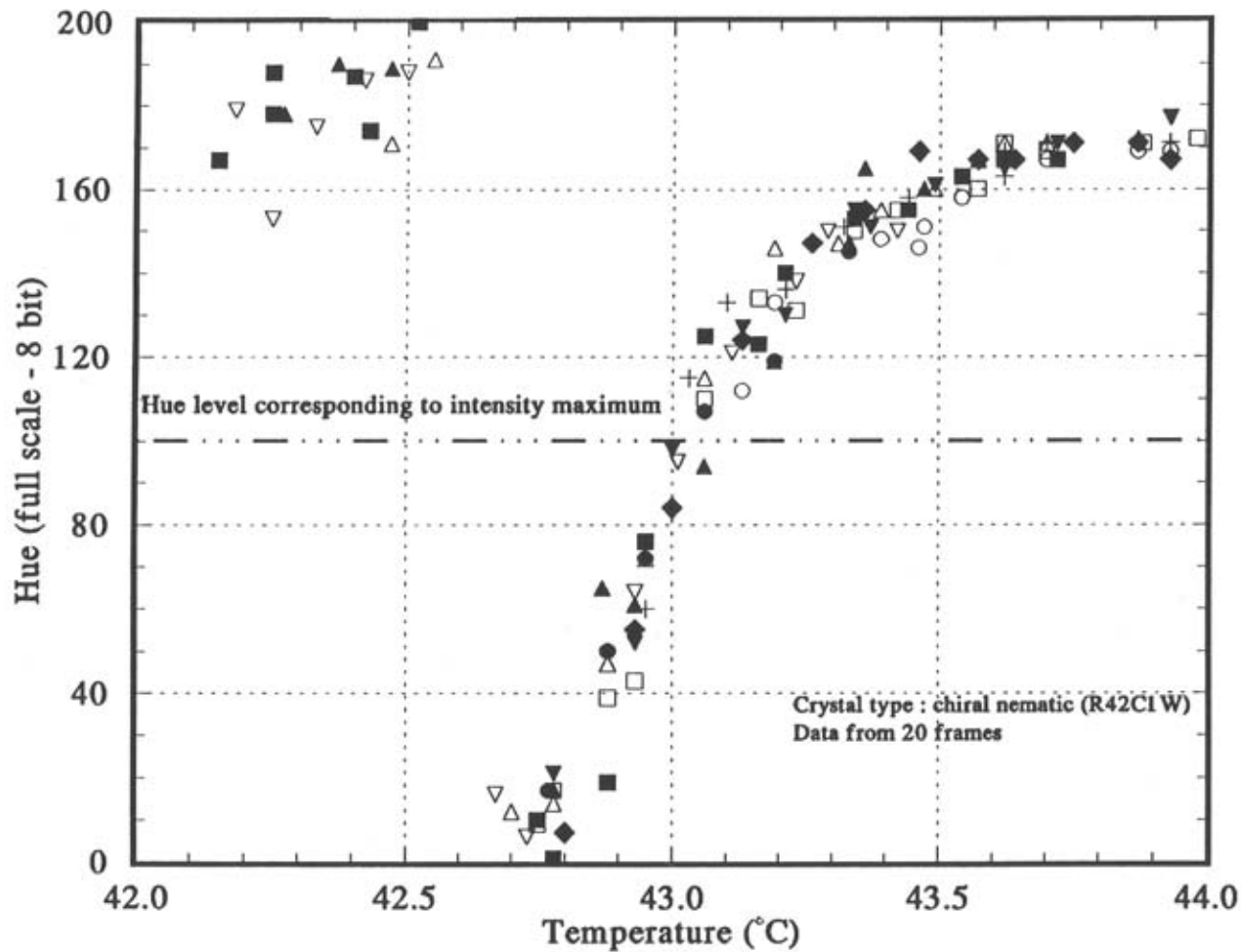


Figure 2.12 Local hue versus temperature curve.

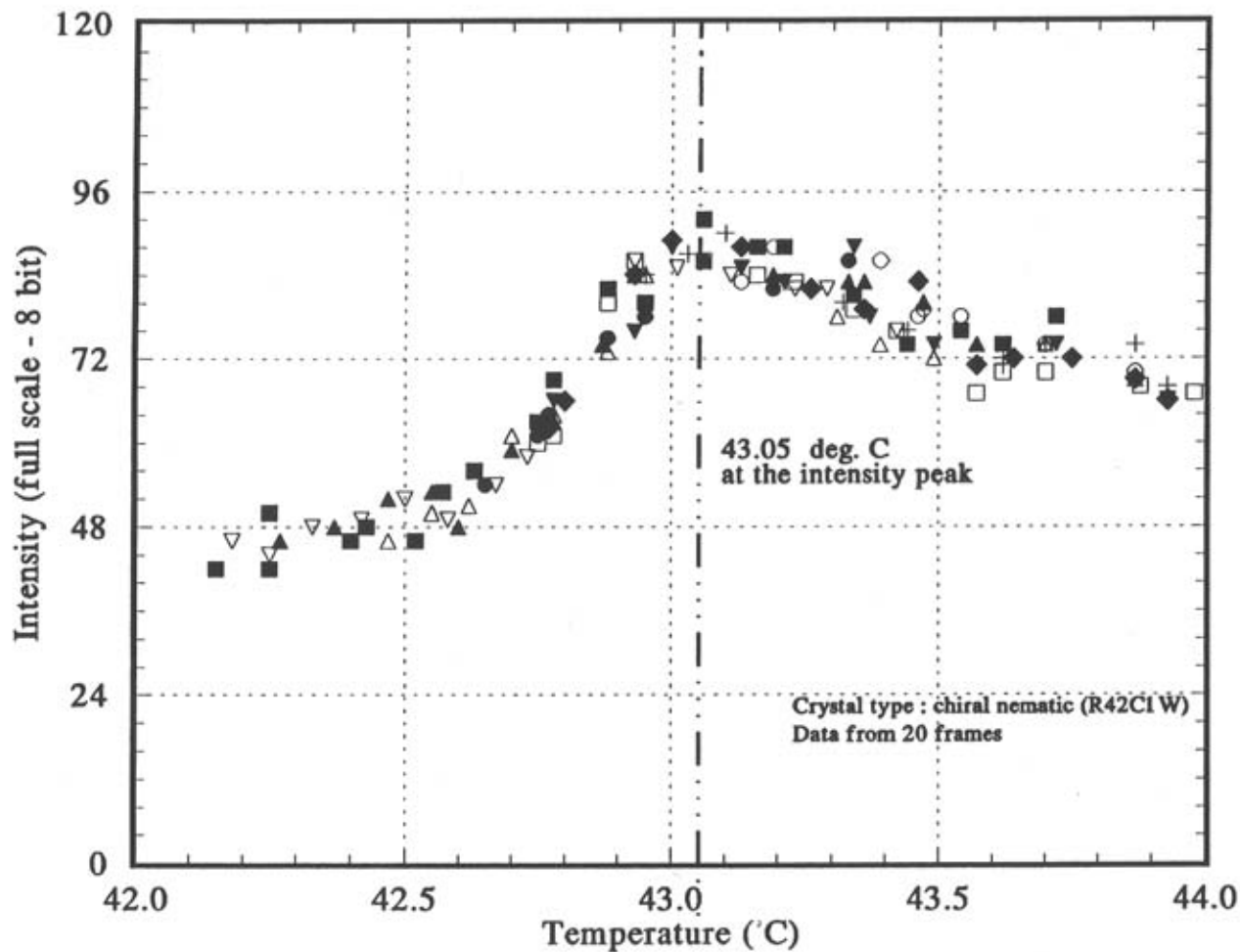


Figure 2.13 Local intensity versus temperature curve.

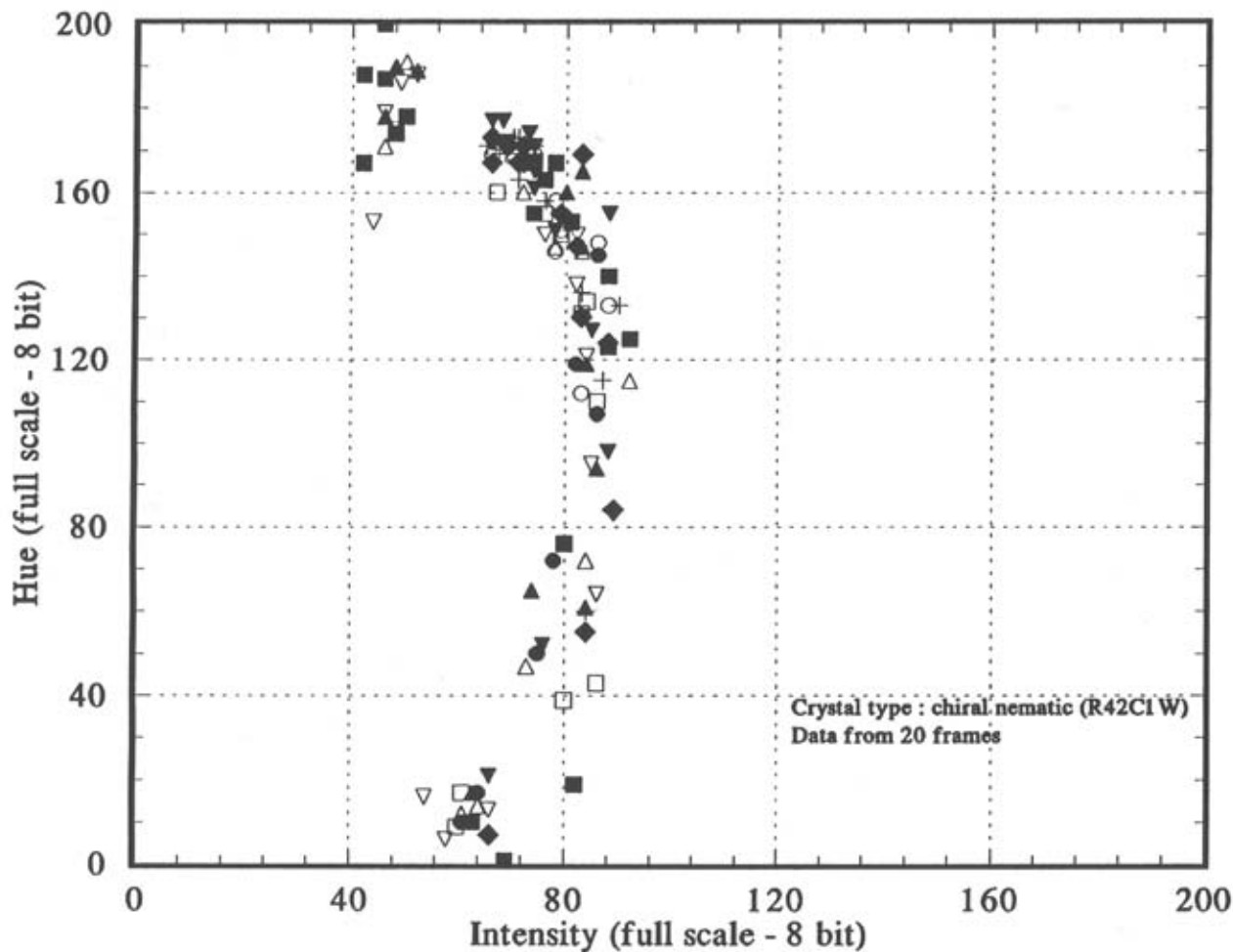


Figure 2.14 Local hue versus local intensity curve.

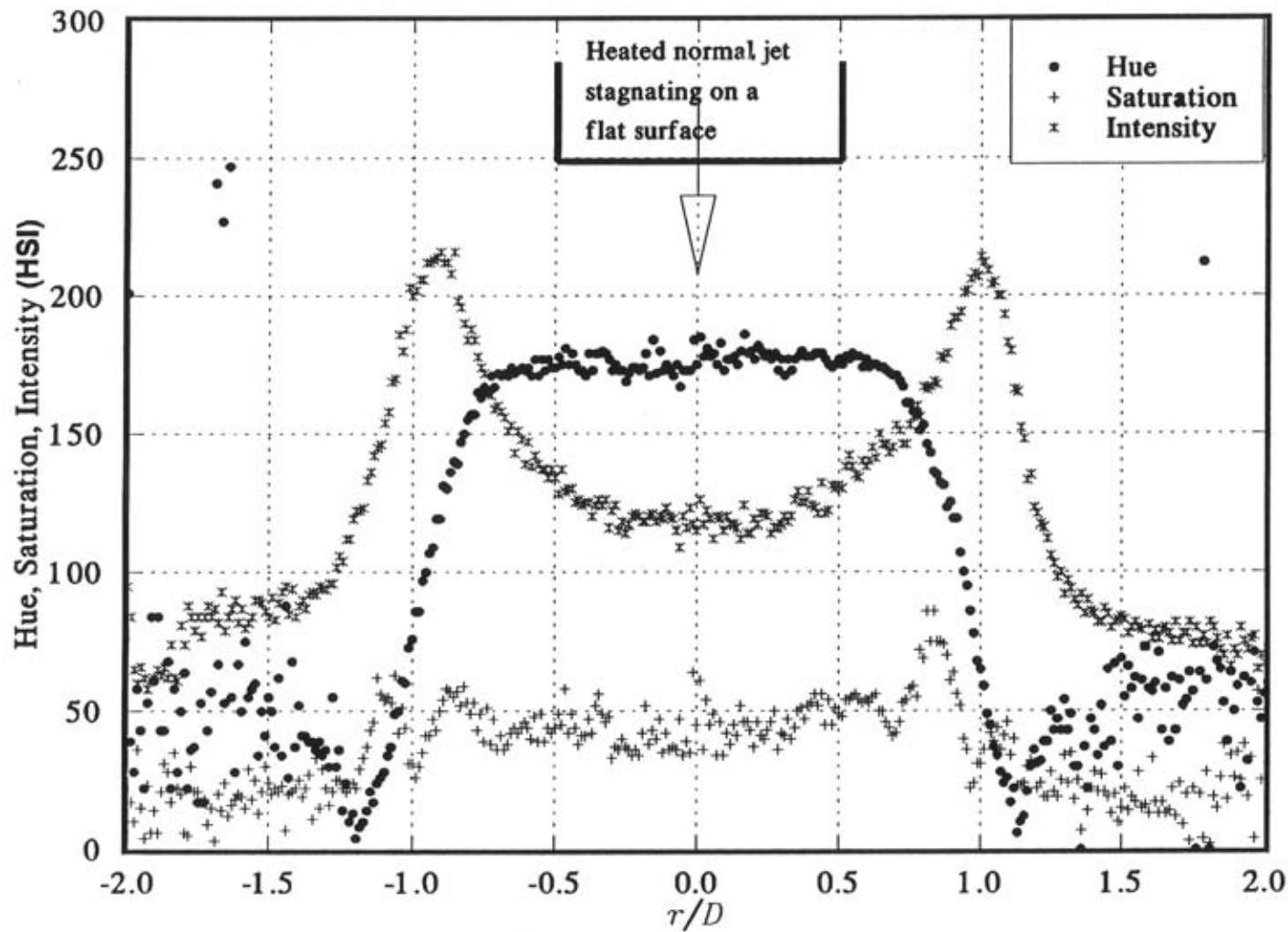


Figure 2.15 H,S,I distributions of the concentric image generated from a heated jet stagnating on a flat plate.

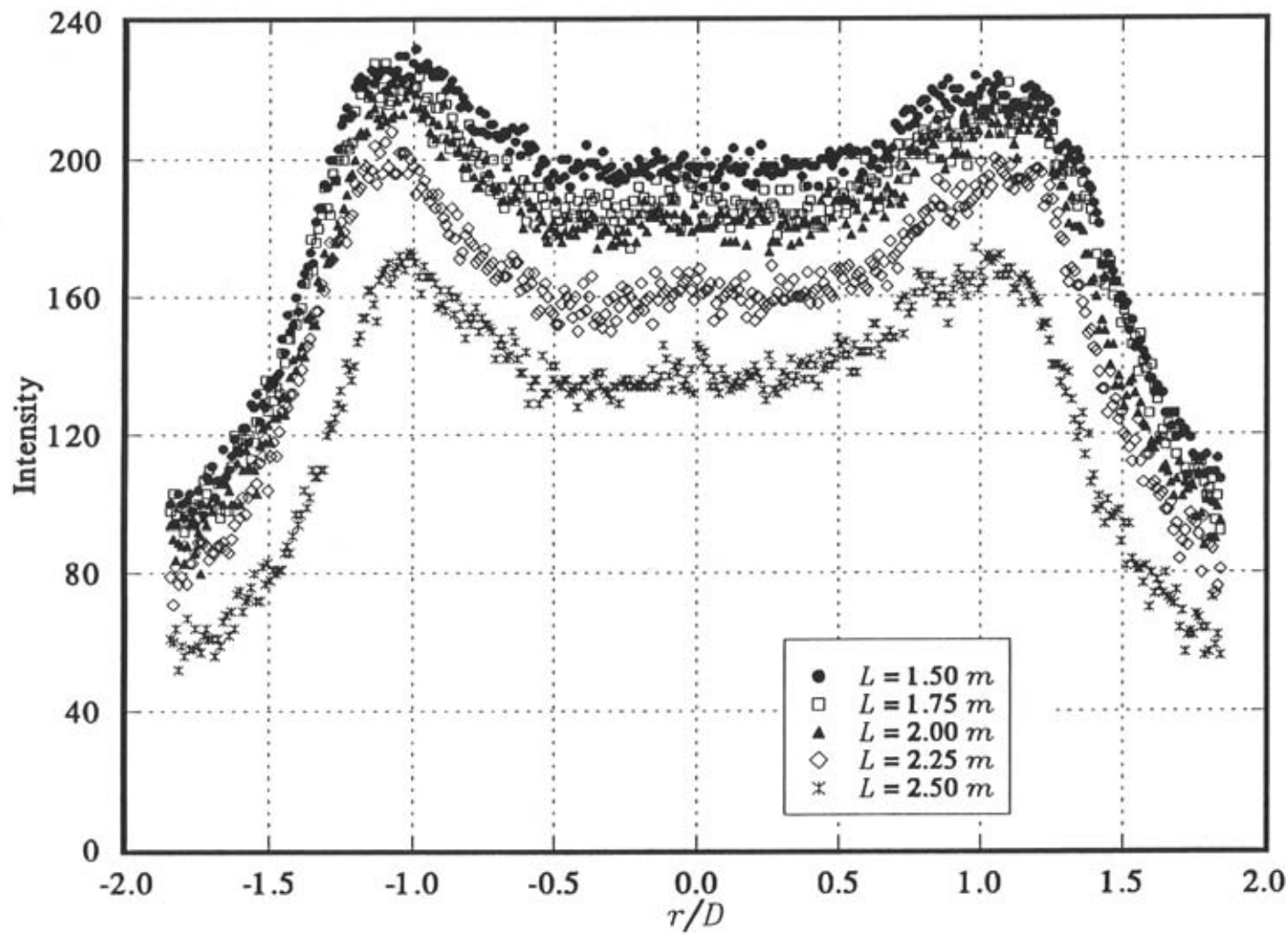


Figure 2.16 Variation of local intensity values under strong illumination level changes.

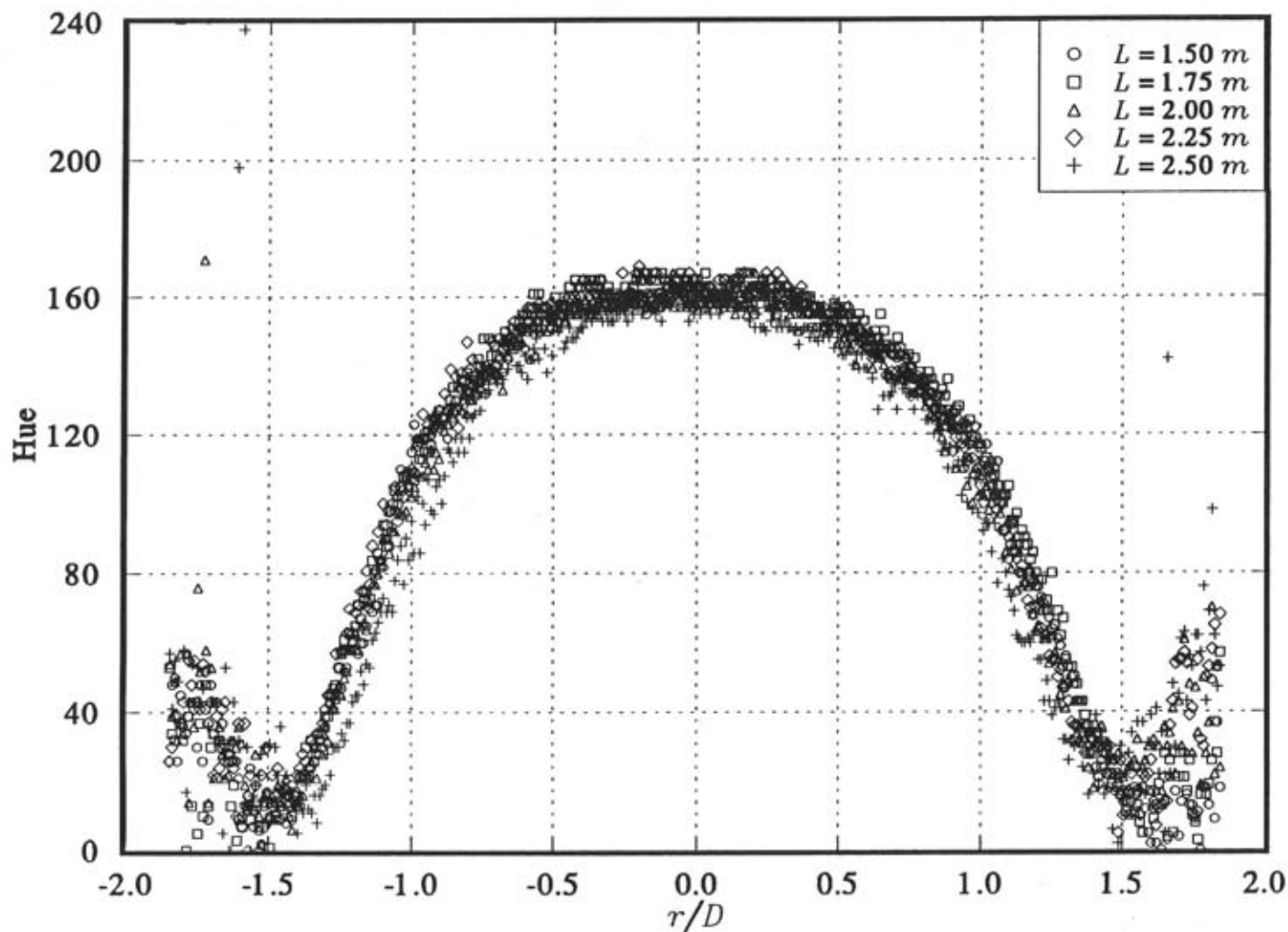


Figure 2.17 Variation of local hue values under strong illumination level changes.

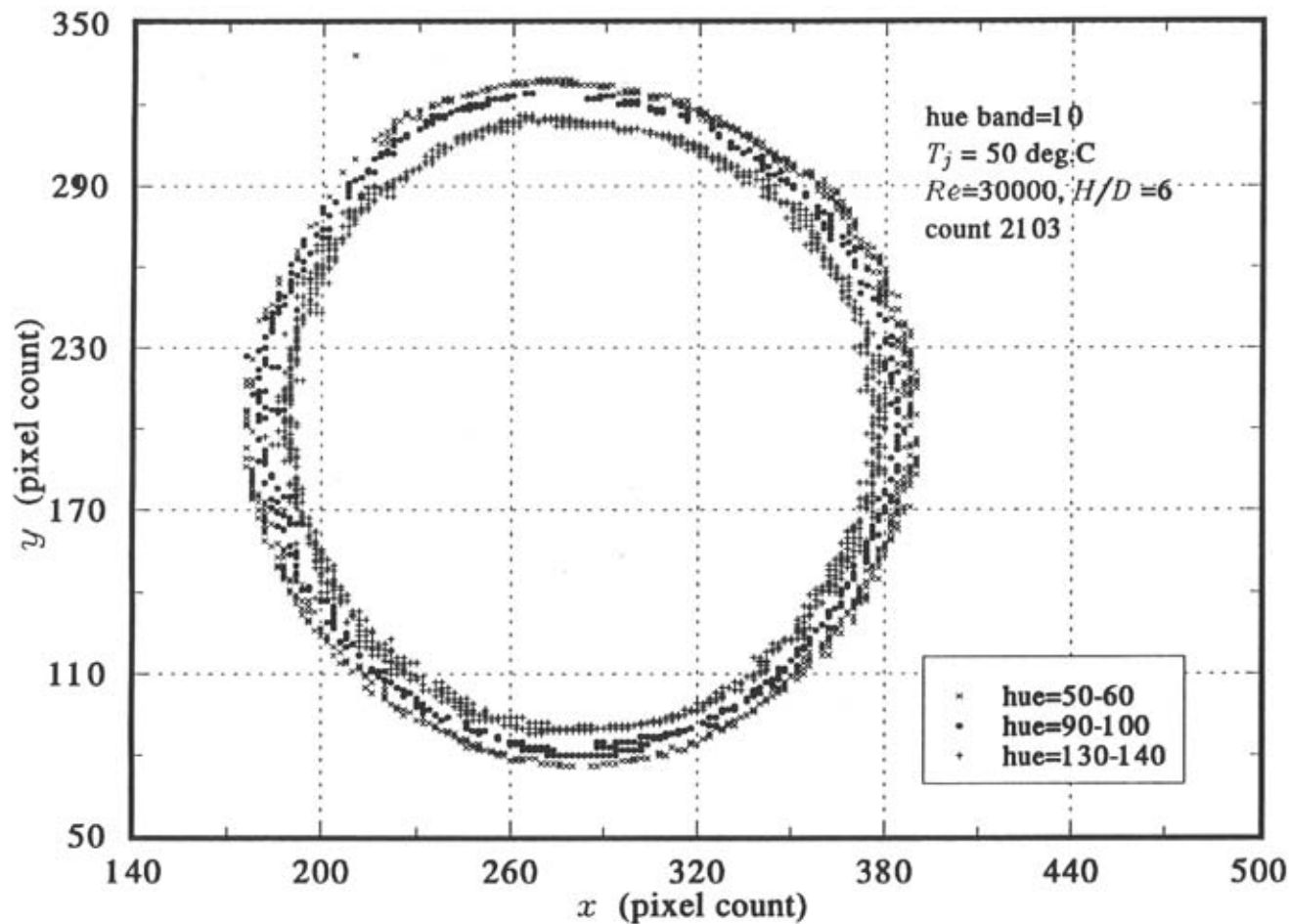


Figure 2.18 Three hue levels (isotherms) mapped using an image processor from a concentric liquid crystal image.